Electrochemical Oxidation of Hexakis(dimethylamino)benzene

Bernd Speiser,* Marc Würde, and Cäcilia Maichle-Mössmer

Dedicated to Professor Hans Schäfer on the occasion of his 60th birthday

Abstract: Hexakis(dimethylamino)benzene is anodically oxidized to its chemically stable dication in an electrochemically slow two-electron process. This redox process was characterized by cyclic voltammetry, chronoamperometry, chronocoulometry, and bulk electrolysis with isolation of the bis(hexafluorophosphate) of the dication. The crystal structure of this dication salt shows considerable distortion, in accord with earlier results for the bis(triiodide). The sluggishness of the electron transfer is related to structural changes during oxidation: two noncoplanar polymethine systems coupled by two long C–C single bonds form. The thermodynamics of the oxidation is characterized by inversion of potentials and disproportionation of a hypothetical radical cation. In contrast to earlier reports, no particular destabilization of the dication is assumed. Further oxidation of the dication proceeds via a tri- to a tetracation in two steps. The tri- and tetracations undergo chemical follow-up reactions.

Keywords: amino compounds · cyclic voltammetry · electrochemistry · electron transfer · potential inversion

Introduction

The oxidation chemistry of hexakis(dimethylamino)benzene (HDMAB, **1**), an extremely electron-rich aromatic compound, has attracted interest over the years.[1–4] It was speculated that the dication of **1**, $\mathbf{1}^{2+}$, might possess a triplet ground state, which in turn would possibly provide a model for compounds forming organic ferromagnetic materials.[1] The dication, however, effectively avoids triplet formation or formation of a delocalized antiaromatic 4 π-electron system by distortion of the six-membered ring.[2] Consequently, ferromagnetic materials, which require at least C_3 symmetry of the basic unit, may not be derived from $\mathbf{1}^{2+}$. The structural change during oxidation, on the other hand, could make **1** an interesting example for the study of distortion effects on electron transfer.

Owing to its electron-richness, **1** was expected to be easily oxidizable. Experimentally determined oxidation potentials were, however, qualified as "more positive than one would predict".[3] This fact was explained by steric strain in the twisted structure of the dication and consequently a decreased stabilization exerted by the six electron-donating nitrogen substituents.[1–4]

Despite the structural characterization of the oxidation product of **1** in the form of its bis(triiodide) $\mathbf{1}^{2+}(I_3^-)_2$,[2] the oxidation mechanism of the neutral compound has not been described without contradictory details. In CH_2Cl_2/0.1 M tetrabutylammonium perchlorate an irreversible oxidation ($E = +0.32$ V vs. Ag/AgCl) was reported.[3] Chemical oxidation with iodine yielded $\mathbf{1}^{2+}(I_3^-)_2$, suggesting a *two*-electron process.[2] Thus, **1** would react similarly to 1,2,4,5-tetrakis(dimethylamino)benzene (**2**), which also forms a dication upon oxidation.[5] Recently, *slow* two-electron oxidations were described for 3,6-bis(dimethylamino)durene (**3**) and 9,10-bis(dimethylamino)anthracene (**4**).[6] Several other amino-substituted benzenes and related compounds behave differently: *N*,*N*,*N*′,*N*′-tetramethyl-*p*-phenylenediamine (**5**),[7,8] 1,3-bis(diarylamino)benzenes,[9] 1,3,5-tris(diisopropylamino)benzene (**6**),[10] as well as other triamino benzene derivatives,[11–14] hexaaminobenzene (**7**),[15] hexaazaoctadecahydrocoronene (HOC, **8**),[16,17] and bis- and tetrakis(dimethylamino)dibenzothiophenes with an appropriate substituent pattern,[18] all undergo successive *one*-electron oxidation steps with clearly separated potentials.

Two reports have appeared which also describe the primary oxidation of **1** as a *one*-electron process. At fast experimental time scales and $T = -50\,^{\circ}C$ in CH_2Cl_2 or liquid SO_2, Dietrich and Heinze observed "monocation" formation at +0.66 V vs. Ag/AgCl,[4] much more positive than described in the earlier report.[3] Chemical oxidation in the presence of acid and irreversible electrochemical oxidation (cyclic voltammetry, first oxidation potential at +0.50 V vs. a saturated calomel electrode, ≈+0.54 V vs. Ag/AgCl) yielded a "radical cation".[19] On the other hand, in solution in CH_2Cl_2 or 1,1,1,3,3,3-hexafluoropropan-2-ol after the oxidation of **1** with Tl^{III}

[*] Prof. Dr. B. Speiser, Dipl.-Chem. M. Würde
Universität Tübingen, Institut für Organische Chemie
Auf der Morgenstelle 18, D-72076 Tübingen (Germany)
Fax: Int. code + (49) 7071 29-6205
e-mail: bernd.speiser@uni-tuebingen.de
Dr. C. Maichle-Mössmer
Universität Tübingen, Institut für Anorganische Chemie

[**] Electrochemistry of Polyaminobenzenes, Part 1.

  0947-6539/98/0402-0222 $ 17.50+.50/0 *Chem. Eur. J.* **1998**, *4*, No. 2

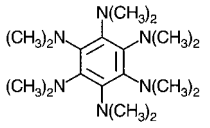
1

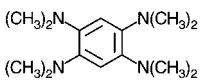
2

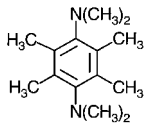
3

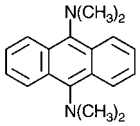
4

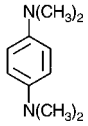
5

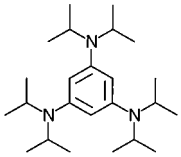
6

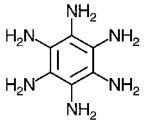
7

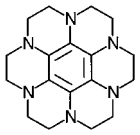
8

trifluoroacetate or 2,3-dichloro-5,6-dicyano-1,4-benzoquinone (DDQ), no ESR signal that could unequivocally be assigned to the corresponding radical cation has yet been detected.[20] In view of these not necessarily consistent results, a first goal of the present study was to define the electron stoichiometry of the primary oxidation step of **1**. We also attempted to complement such results by an electrochemical characterization of the oxidation product.

Recently, the possibility of two-electron redox processes involving organic compounds was debated,[6,21–23] in particular for cases where considerable structural changes during electron transfer (ET) are expected. In this regard, we also became interested in detailed mechanistic information for the electrochemical oxidation of **1**. Changes of molecular structure occurring in concert with an ET reaction may result in large inner reorganisation energies λ_i,[24] with a concomitant decrease of the ET rate constant. Thus, the apparent positive shift of the HDMAB oxidation peak potential may possibly be controlled by kinetic properties and be due to a slow (quasireversible) ET reaction rather than to a thermodynamically unfavorable process. Several organic compounds bearing amino nitrogen substituents show slow ET due to large λ_i.[6,21,24–27] Moreover, in the case of two-electron processes with structural changes, inversion of potentials[27] is known to occur if the transfer of the second electron is thermodynamically easier than that of the first. The present paper will provide electrochemical evidence for kinetic control of the HDMAB oxidation (quasireversible ET) and inversion of potentials. It will also show that at least two further oxidation states can be formed by electrochemical oxidation processes, and will thus give a detailed mechanistic characterization of the electrochemical oxidation of HDMAB.

Abstract in German: *Hexakis(dimethylamino)benzol wird anodisch in einem langsamen Zweielektronenprozeß zu seinem chemisch stabilen Dikation oxidiert. Dieser Redoxprozeß wurde durch Cyclovoltammetrie, Chronoampero- und Chronocoulometrie sowie die präparative Elektrolyse charakterisiert, die zur Isolierung des Bis(hexafluorophosphats) des Dikations führte. Die Kristallstruktur des Dikationsalzes zeigt in Übereinstimmung mit früheren Ergebnissen für das Bis(triiodid) erhebliche Strukturverzerrungen. Die Verlangsamung des Elektronentransfers steht im Zusammenhang mit strukturellen Veränderungen während der Oxidation (Bildung zweier nicht-koplanarer Polymethinsysteme, die über zwei lange C–C-Einfachbindungen miteinander verknüpft sind). Die Thermodynamik der Oxidation zeichnet sich durch Potentialinversion und Disproportionierung eines hypothetischen Radikalkations aus. Im Gegensatz zu früheren Arbeiten wird keine ausgeprägte Destabilisierung des Dikations angenommen. Die weitere Oxidation des Dikations verläuft über ein Tri- zu einem Tetrakation in zwei getrennten Schritten. Das Tri- und das Tetrakation gehen chemische Folgereaktionen ein.*

Results and Discussion

Cyclic voltammetry (CV) of 1: HDMAB (**1**) is soluble in CH_3CN only in small concentrations. Cyclic voltammetric signals in this solvent were weak. On the other hand, the compound is easily soluble in CH_2Cl_2, but cyclic voltammograms in dichloromethane electrolytes showed appreciable effects of adsorption at the electrode (Figure 1). This is

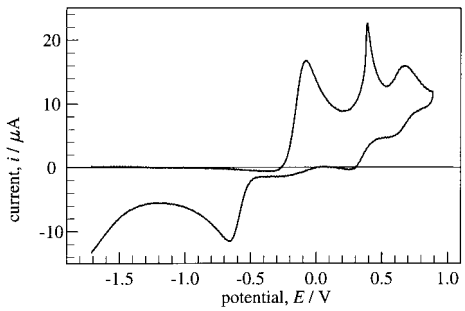

Figure 1. Cyclic voltammogram of hexakis(dimethylamino)benzene **1** in CH_2Cl_2/0.1 M NBu_4PF_6, $v = 1.0\ V\,s^{-1}$, $c = 0.18$ mM at a Pt tip electrode and at ambient temperature.

probably due to the low solubility of the primary oxidation product of **1** in CH_2Cl_2. Since adsorption would severely hamper the detailed analysis of the cyclic voltammograms, we settled on a 1:1 (v/v) mixture of CH_3CN and CH_2Cl_2 as the solvent for most of the ensuing experiments. In electrolytes based on this mixture, after background subtraction, excellent cyclic voltammetric signals could be obtained in which interference of adsorption effects was minimized.

Cyclic voltammograms of **1** in CH_3CN/CH_2Cl_2/0.1 M NBu_4PF_6 spanning the accessible potential window in the positive potential region at various scan rates v and concentrations c give an overview of the redox chemistry of the starting compound (Figure 2a–c). The oxidation of **1** under

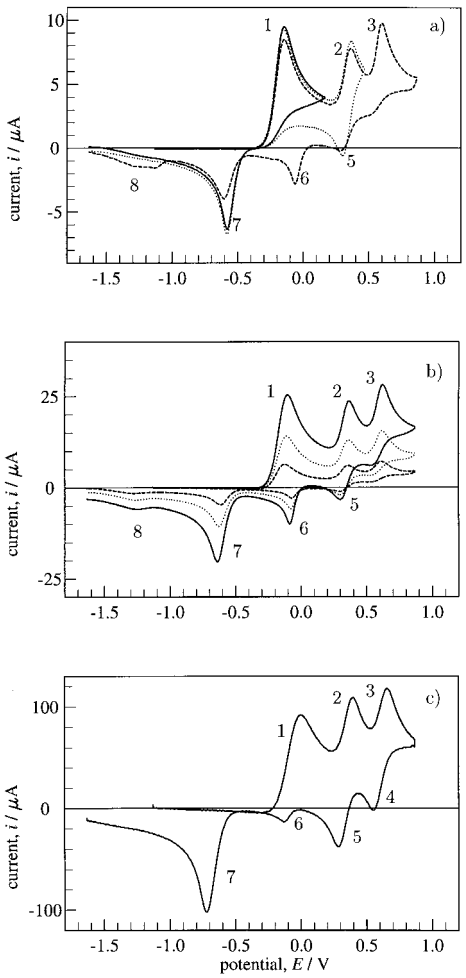

Figure 2. Cyclic voltammograms of hexakis(dimethylamino)benzene **1** in CH_3CN/CH_2Cl_2 (1:1, v/v)/0.1 M NBu_4PF_6, variation of scan rate v and concentration c. a) $v = 0.1\ V s^{-1}$, $c = 0.24$ mM, $E_\lambda = +0.166$ (—), $+0.466$ (····), $+0.866$ (- - - -) V; b) $v = 1.0\ V s^{-1}$, $c = 0.06$ (- - - -), 0.12(····),0.24 mM (—); c) $v = 20\ V s^{-1}$, $c = 0.24$ mM; Pt tip electrode, ambient temperature.

these conditions is characterized by three peaks, 1–3. An increase in the concentration does not cause peaks to appear or disappear (Figure 2b). All peak currents are proportional to the concentration of **1**.

In peak 1 primary oxidation occurs. At high scan rates in particular, peak 1 broadens compared with peaks 2 and 3 and decreases in relative height ($v = 20\ V s^{-1}$, Figure 2c). This indicates that electron transfer in peak 1 is relatively slow. Also at high scan rates, reduction peaks 4 and 5 become clearly visible (related to oxidation signals 3 and 2, respectively; Figure 2c). For slower time scales ($v = 0.1$ and $1.0\ V s^{-1}$, Figures 2a and b), peak 4 disappears and peak 5 considerably decreases in intensity. Simultaneously, reduction peak 6 increases. Reduction signal 7 is intense, but relatively narrow. Signal 8 is only observed at lower scan rates and after passage of peak 3. It is thus related to the product formed at more positive potentials and may be due to some remaining adsorption process. It is, however, strongly shifted from the other peaks and does not interfere with their interpretation.

Peak 1 shifts to more positive potentials with increasing v, as expected for a slow ET. Also, a shift to more positive values of E_p^1 is observed with increasing c (Table 1). The behavior of E_p^2 (see Table 1 and discussion below) shows that this can not be due to effects of uncompensated resistance. The half-peak width $|E_p^1 - E_{p/2}^1|$ is independent of c, but increases with v, consistent with the hypothesis of a slow ET.

Table 1. Peak potential features in cyclic voltammograms of **1**.

v /V s^{-1}	E_p^1 /V			$\lvert E_p^1 - E_{p/2}^1 \rvert$ /V[a]	E_p^2 /V[a]	E_p^3 /V[a]
	$c = 0.06$	0.12	0.24 mM			
0.02	−0.190	−0.182	−0.175	0.066	+0.361	+0.578
0.05	−0.177	−0.167	−0.150	0.067	+0.362	+0.589
0.1	−0.167	−0.154	−0.147	0.069	+0.360	+0.592
0.2	−0.153	−0.143	−0.129	0.073	+0.360	+0.600
0.5	−0.137	−0.123	−0.109	0.067	+0.362	+0.613
1.0	−0.128	−0.108	−0.092	0.077	+0.361	+0.616
2.0	−0.103	−0.092	−0.068	0.083	+0.363	+0.616
5.12	−0.075	−0.063	−0.033	0.092	+0.364	+0.628
10.24	−0.052	−0.039	−0.009	0.098	+0.371	+0.627
20.48	−0.032	−0.009	+0.025	0.105	+0.383	+0.635

v /V s^{-1}	$\Delta E_p^{2/5}$ /V[a]	$\Delta E_p^{3/4}$ /V[a]	E_p^7 /V		
			$c = 0.06$	0.12	0.24 mM
0.02	0.075	–[b]	−0.522	−0.526	−0.541
0.05	0.080	–[b]	−0.546	−0.555	−0.583
0.1	0.062	–[b]	−0.567	−0.581	−0.597
0.2	0.063	–[b]	−0.578	−0.590	−0.615
0.5	0.061	–[b]	−0.597	−0.608	−0.632
1.0	0.061	0.090	−0.607	−0.622	−0.651
2.0	0.063	0.082	−0.625	−0.635	−0.677
5.12	0.075	0.077	−0.650	−0.659	−0.708
10.24	0.078	0.076	−0.676	−0.679	−0.731
20.48	0.092	0.084	−0.702	−0.709	−0.753

[a] Independent of c, mean values over data at $c = 0.06$, 0.12, 0.24 mM. [b] Not observed owing to absence of peak 4.

Experiments with a switching potential of $E_\lambda = +0.166$ V, that is, one between oxidation peaks 1 and 2 (Figure 2a, solid line), reveal that peak 7 has to be assigned to the reduction of the product generated in peak 1: peaks 1 and 7 form a peak couple despite their considerably enhanced potential difference ($\Delta E_p > 0.4$ V at $v = 0.1\ V s^{-1}$, $\Delta E_p > 0.6$ V at $v = 2.0\ V s^{-1}$). The reason for this behavior will be discussed below. Like E_p^1, peak potential E_p^7 depends on v and c.

Peak current function $i_p^1/\sqrt{v}c$ (Table 2) decreases slightly with increasing scan rate, again consistent with the hypothesis of a slow ET. Peak current i_p^7 is proportional to the square root of the scan rate for $v > 0.1\ V s^{-1}$, excluding involvement of adsorption processes (Table 2). Only for small v does $i_p^7/\sqrt{v}c$ decrease; we attribute this to the long time delay between passage of peaks 1 and 7 in these experiments. At small scan rates a fraction of the primary oxidation product escapes reduction on the reverse scan due to nonideal edge diffusion into the bulk solution.

Voltammograms with $E_\lambda = +0.466$ V (Figure 2a, dotted line) prove that peak 5 corresponds to the reduction of the oxidation product formed in peak 2. Peak potential E_p^2 is essentially independent of v and c, with $\Delta E_p^{2/5} = 0.066 \pm 0.009$ V for scan rates up to $v = 5.0\ V s^{-1}$ (Table 1). Only for $v > 5.0\ V s^{-1}$ do the two peaks shift apart. The peak current function $i_p^2/\sqrt{v}c = (59 \pm 6)\ A cm^3 s^{1/2} V^{-1/2} mol^{-1}$ (i_p^2 referred to the current decreasing from peak 1; Table 2) is independent of

0947-6539/98/0402-0224 $ 17.50+.50/0 *Chem. Eur. J.* **1998**, *4*, No. 2

Table 2. Peak current features in cyclic voltammograms of **1**.

v /V s^{-1}	$i_p^1/\sqrt{v}c$[a]	$i_p^7/\sqrt{v}c$[a]	$i_p^2/\sqrt{v}c$[a,b]	$i_p^6/\sqrt{v}c$[a,c]
0.02	116	26	63	8.9
0.05	138	40	59	4.1
0.1	128	75	65	41
0.2	126	77	64	47
0.5	121	81	59	51
1.0	143	83	58	47
2.0	116	84	57	41
5.12	111	88	56	30
10.24	106	84	58	22
20.48	104	84	59	11

[a] In A s$^{1/2}$ cm^3 V$^{-1/2}$ mol^{-1}, independent of c, mean values over data at $c =$ 0.06, 0.12, 0.24 mM. [b] Determined with extrapolated current from peak 1 as baseline. [c] i_p^6 referred to zero current.

v and c. Peaks 2 and 5 are assigned to oxidation and reduction of two species related by a one-electron redox process with a mid-point potential of $\bar{E}^{2/5} = +0.330 \pm 0.005$ V. This process is reversible at small v, becoming quasireversible at larger v. Independence of $\Delta E_p^{2/5}$ on c for $v \leq 10$ V s^{-1} proves that uncompensated iR drop may only obscure the voltammetric curves above this scan rate.

For $E_\lambda = +0.866$ V and after passage through oxidation peak 3, the remaining reduction peaks 4 and 6 are observed. At scan rates $v \geq 1.0$ V s^{-1}, peak 4 is clearly present and again indicates a one-electron redox step with quasireversibility being noticeable at $v \geq 5.0$ V s^{-1} (shift of E_p^3, Table 1; $\Delta E_p^{3/4} \approx$ 0.08 V; $\bar{E}^{3/4} = +0.584 \pm 0.010$ V). With decreasing scan rate, peak 4 decreases in intensity and disappears at $v < 1.0$ V s^{-1}. The oxidation product formed in peak 3 undergoes an irreversible chemical follow-up reaction. The shift of peak 3 to less positive potentials at $v < 1.0$ V s^{-1} is in accordance with this hypothesis (Table 1).

The scan rate at which peak 4 disappears is independent of the substrate concentration. Consequently, the follow-up reaction must be of first or pseudo-first order. Peak current i_p^3 in voltammograms of **1** is not further analyzed, since the errors in separation of the current contribution of the third electron transfer reaction are large.

The product of the chemical reaction is reduced in peak 6, whose peak current function increases with a decrease of v (Table 2). At scan rates below 0.1 V s^{-1} $i_p^6/\sqrt{v}c$ strongly decreases. Possibly, a further chemical reaction becomes dominant on this time scale, and in turn destroys the species reduced in peak 6. The position of peak 6 depends on c. We will not further discuss the behavior of peak 6 in detail here.

Chronoamperometry (CA) and chronocoulometry (CC) of 1: The peak broadening observed for peak 1 precludes comparison of the peak current functions of the oxidation peaks and derivation of the electron stoichiometry for the oxidation of **1** from cyclic voltammograms. Potential step techniques such as chronoamperometry and chronocoulometry, on the other hand, usually investigate the electron transfer at a potential which is in the mass-transfer limited current region.[28] Thus, even systems with sluggish electron-transfer steps may be rendered diffusion-controlled under these conditions because of the increased driving force for the ET. Effects of quasireversibility become negligible, at least on longer time-scales, and the relative numbers of electrons transferred in successive steps can be determined.

CA and CC were used to characterize the oxidation of **1** at potentials between peaks 1 and 2 ($E = +0.166$ V), between peaks 2 and 3 ($E = +0.466$ V), and at potentials positive of peak 3 ($E = +0.866$ V). The time scale was varied through the pulse width τ. Table 3 gives results for the slope of the Anson plot, $Q/\sqrt{tc}$, from CC experiments and the Cottrell constant,

Table 3. Chronocoulometric and chronoamperometric results for oxidation of **1** at different values of E (in V).[a]

E/V τ /s	+0.166	+0.466	+0.866
$Q/\sqrt{tc}$[b]			
0.1	0.0515	0.0803	0.104
1.0	0.0522	0.0775	0.101
10.0	0.0576	0.0879	0.107
$(Q/\sqrt{tc})/(Q/\sqrt{tc})_{E=+0.166\,V}$			
0.1	1.000	1.56	2.02
1.0	1.000	1.48	1.93
10.0	1.000	1.53	1.86
$Q(2\tau)/Q(\tau)$			
0.1	0.40 ± 0.01	0.45 ± 0.05	0.43 ± 0.04
1.0	0.42 ± 0.01	0.43 ± 0.03	0.46 ± 0.03
10.0	0.49 ± 0.01	0.51 ± 0.02	0.59 ± 0.03
$i/\sqrt{tc}$[c]	30.0	41.2	54.8
$(i\sqrt{t/c})/(i\sqrt{t/c})_{E=+0.166\,V}$	1.00	1.37	1.83

[a] Mean values from experiments at $c = 0.06$, 0.12, and 0.24 mM. [b] In C cm^3 s$^{-1/2}$ mol^{-1}. [c] In A cm^3 s$^{-1/2}$ mol^{-1}, mean values from all τ.

$i\sqrt{tc}$, from CA experiments. Both quantities should be proportional to the number of electrons transferred,[28] n. Also, results for the ratio $Q(2\tau)/Q(\tau)$ from CC are shown. For an ET without follow-up reaction, this ratio is expected to approach 0.414.[29]

With increasing potential, both the Cottrell constants and the Anson plot slopes increase. If we divide the data by the respective result at $E = +0.166$ V, the relative values correspond to a ratio of 1:1.48:1.91 (mean values over all τ, and over CC and CA data). Since numbers of transferred electrons must be integers, this result indicates that the n values for the three successive oxidation steps form a ratio of 2:3:4. Hence, in the first electrochemical step two electrons are transferred. In full accordance with the results of the CV experiments, in each of the two further steps one electron is exchanged. Consequently, while in peak 1 a dication $\mathbf{1}^{2+}$ is produced, a trication $\mathbf{1}^{3+}$ and a tetracation $\mathbf{1}^{4+}$ are formed in peaks 2 and 3, respectively.

The $Q(2\tau)/Q(\tau)$ ratios in Table 3 are close to 0.414 for $E = +0.166$ and $+0.466$ V at $\tau = 0.1$ and 1.0 s, but increase for $E = +0.866$ V and with increasing τ. This indicates that some material generated at the potential of peak 3 disappears and cannot be re-reduced in the second part of the CC experiment. Again, this is in accordance with the CV data, indicating a follow-up reaction coupled to the ET in peak 3: the tetracation $\mathbf{1}^{4+}$ is not stable at slower time scales. At $\tau = 10$ s, some product may once more be lost due to edge diffusion

into the bulk solution causing $Q(2\tau)/Q(\tau)$ to deviate from 0.414 even at $E = +0.166$ and $+0.466$ V.

Preparative scale electrolysis and coulometry of 1: HDMAB was anodically oxidized at potentials between peaks 1 and 2 in preparative scale electrolysis experiments in both the CH_3CN/CH_2Cl_2 mixture and in CH_2Cl_2. During electrolysis, the solution turned from colorless to dark brown. The charge passed during oxidation corresponded to 2 electrons per molecule of **1** present in the starting solution, confirming that a dication was formed.

During electrolysis in CH_2Cl_2 a black solid precipitated. It was identified as the bis(hexafluorophosphate) of the dication, $\mathbf{1}^{2+}(PF_6^-)_2$, by ^1H and ^{13}C NMR spectroscopic results (both compared with results for the bis(triiodide) of $\mathbf{1}^{2+}$[2]) as well as elemental analysis. The limited solubility of the dication in CH_2Cl_2 is probably the reason for the adsorption effects observed in the voltammograms of **1** in this solvent.

In CH_3CN/CH_2Cl_2 no precipitate formed. Peak 1 did not appear in the CV of the oxidized solution: the starting compound had completely disappeared (Figure 3). However,

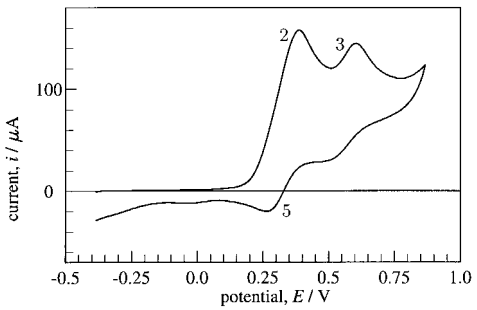

Figure 3. Cyclic voltammogram in solution of **1** in CH_3CN/CH_2Cl_2 (1:1, v/v)/0.1 M NBu_4PF_6, after electrolysis at $+0.166$ V; $c(\mathbf{1}) = 10$ mM in starting solution; $v = 0.1$ V s^{-1}; Pt tip electrode, $T = 17\,^\circ$C.

peaks 2 and 3 observed in the voltammogram of **1** were still present. After the potential had been scanned to values more negative than peak 7, peak 1 reappeared on the reverse oxidation scan.

During preparative-scale reduction of the oxidized solution the deep color disappeared, the precipitate redissolved in CH_2Cl_2, and again 2 F mol^{-1} of **1** were transferred. The potential of the working electrode had to be set to rather negative potentials ($E \approx -1.7$ V in CH_2Cl_2 and ≈ -1.6 V in CH_3CN/CH_2Cl_2) to achieve reduction. In voltammograms, after such a reduction peak 1 was already present during the first oxidation scan. On the basis of these bulk electrolysis and CV experiments we conclude that, while being *electrochemically quasireversible* (transfer of at least one electron is slow compared with diffusional transport), oxidation of **1** to its dication is *chemically reversible*, that is, the oxidation product $\mathbf{1}^{2+}$ is stable and can be reduced to the neutral starting compound.

Crystal structure of $\mathbf{1}^{2+}(PF_6^-)_2$: X-ray crystallographic results for the structure of $\mathbf{1}^{2+}$ bis(triiodide) have already been reported.[2] Although the structure determination was carried out with crystals of only "mediocre"[2] quality, the main features of the dication conformation could be described. However, the data include some large temperature factors, and the unit cell [$a = 16.243(5)$, $b = 11.051(4)$, $c = 20.358(7)$ Å, $\beta = 112.02(3)^\circ$, $Z = 4$] and the space group ($P2/c$) may not be consistent. A *C*-centered cell may be an alternative to the primitive one.

Since $\mathbf{1}^{2+}(PF_6^-)_2$ was obtained in good quality crystals, we reexamined the solid-state dication structure with the product prepared electrochemically in the present work. As with the structure described for $\mathbf{1}^{2+}(I_3^-)_2$,[2] the benzene ring of the dication in the bis(hexafluorophosphate) attains a twisted conformation (Figure 4). The molecule is composed of two

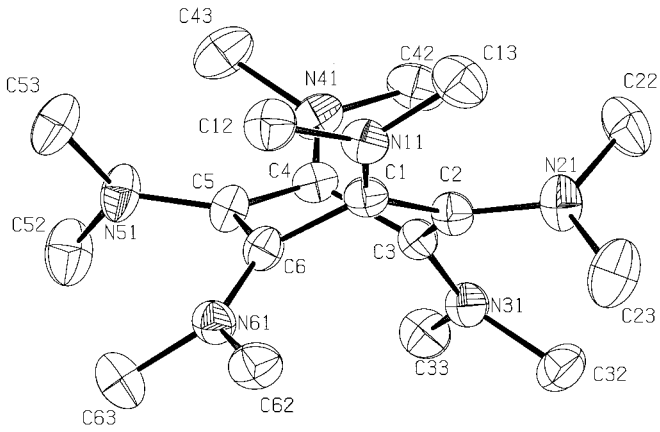

Figure 4. Structure of the hexakis(dimethylamino)benzene dication in $\mathbf{1}^{2+}(PF_6^-)_2$ crystals.

nearly planar delocalized polymethine systems[30] consisting of three carbon ring atoms and two $N(CH_3)_2$ groups each. The central carbon atom of each polymethine chain is substituted by an additional $N(CH_3)_2$ group. The angle between these two systems is 34.37°. The bond distances in the two systems (N11-C1-C2-C3-N31 and N41-C4-C5-C6-N61) are very similar (Table 4). Electron delocalization results in considerable shortening of the C–N bonds involved in the polymethine systems. In contrast, the bond between one of the central carbons in the polymethine chain (e.g., C2) and the attached nitrogen (N21) is clearly longer. The two C–C bonds coupling the polymethine moieties have single-bond character, as shown by a C–C distance of 1.519 Å. Bond lengths obtained for the bis(hexafluorophosphate) are in good agreement with AM1-calculated distances (Table 4).[2]

Table 4. Selected bond lengths in $\mathbf{1}^{2+}(PF^-_6)_2$ compared with X-ray crystallographic results and AM1-calculated values for the bis(triiodide).[2]

	$\mathbf{1}^{2+}(PF_6^-)_2$	$\mathbf{1}^{2+}(I_3^-)_2$[2]	calcd[2]
C1 – N11	1.329(4)	1.34(3)	1.337(0)
C1 – C2	1.411(4)	1.38(3)	1.439(1)
C2 – N21	1.400(4)	1.43(3)	1.398(0)
C2 – C3	1.435(4)		
C3 – N31	1.313(4)		
C1 – C6	1.519(4)	1.57(5)	1.526(2)

0947-6539/98/0402-0226 $ 17.50+.50/0 *Chem. Eur. J.* **1998**, *4*, No. 2

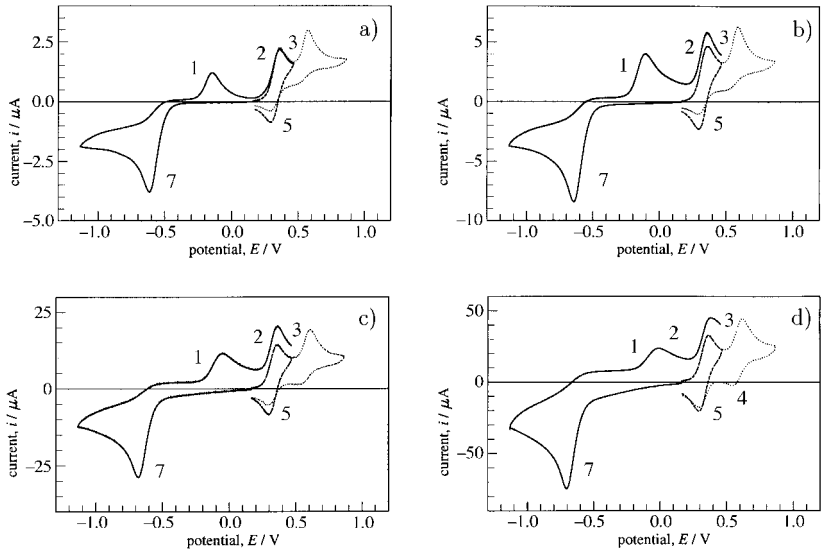

Figure 5. Cyclic voltammograms of $\mathbf{1}^{2+}(PF_6^-)_2$ in CH_3CN/CH_2Cl_2 (1:1, v/v)/0.1M NBu_4PF_6, $c = 0.208$ mM: a) $v = 0.02\ V s^{-1}$; b) $v = 0.1\ V s^{-1}$; c) $v = 1.0\ V s^{-1}$; d) $v = 5.0\ V s^{-1}$ (oxidation cycles to +0.466 V: - - - -, to +0.866 V: ····; reduction cycles: —).

Cyclic voltammetry of $\mathbf{1}^{2+}(PF_6^-)_2$; oxidation: CV of solutions of $\mathbf{1}^{2+}(PF_6^-)_2$ in the CH_3CN/CH_2Cl_2 electrolyte (Figure 5) confirms the mechanistic picture gained so far and gives additional information. No current is observed in solutions of the bis(hexafluorophosphate) of $\mathbf{1}^{2+}$ at a starting potential of +0.166 V. At more positive potentials, the dication is oxidized in two successive one-electron steps (Figure 5, broken and dotted lines; $\Delta E_p^{2/5} = 0.068 \pm 0.005$ V, $\Delta E_p^{3/4} = 0.081 \pm 0.017$ V; Table 5). The peak potential E_p^2 is independent of v and c up to $v = 10.24\ V s^{-1}$. On the other hand, E_p^3 shifts to less positive values at low v, as observed before when starting from **1**, confirming the effect of a follow-up reaction of the tetracation. Again, peaks 2–5 allow the determination of mid-point potentials ($\bar{E}^{2/5} = +0.329 \pm 0.002$, $\bar{E}^{3/4} = +0.582 \pm 0.009$ V), which are in excellent agreement with those obtained from voltammograms of **1**. Only at high scan rates does quasireversibility show up in both cases (indicated by increasing ΔE_p and a shift of E_p above $v = 10.24\ V s^{-1}$). At low scan rates, peak 4 disappears, again owing to an irreversible follow-up reaction of $\mathbf{1}^{4+}$.

From the experiments with both **1** and $\mathbf{1}^{2+}(PF_6^-)_2$ we calculate $E^0(\mathbf{1}^{2+}/\mathbf{1}^{3+}) = +0.330 \pm 0.005$ V and $E^0(\mathbf{1}^{3+}/\mathbf{1}^{4+}) = +0.58 \pm 0.01$ V as the formal potentials of the two consecutive one-electron transfer reactions.

The baseline for i_p^2 is clearly defined in these voltammograms, and for $0.05 \le v \le 10.24\ V s^{-1}$ the current function $i_p^2/\sqrt{v}c$ can be determined to be $(53 \pm 2)\ A cm^3 s^{1/2} V^{-1/2} mol^{-1}$ (Table 6). From the peak currents i_p^2 we calculated the diffusion coefficient of $\mathbf{1}^{2+}$ in CH_3CN/CH_2Cl_2 as $D(\mathbf{1}^{2+}) = 8.2 \times 10^{-6}\ cm^2 s^{-1}$. The peak current ratio i_p^5/i_p^2 in voltammograms of $\mathbf{1}^{2+}$ with $E_\lambda = +0.466$ V is 1.0 ± 0.1, independent of v ($0.05 \le v \le 10.24\ V s^{-1}$), confirming stability of $\mathbf{1}^{3+}$ on the timescale used. Peak current i_p^3 can be estimated if we use the extrapolated current decreasing from peak 2 as the baseline. A ratio of $i_p^3/i_p^2 = 0.8 \pm 0.1$ is found, in accordance with the assumption of two one-electron transfers in peaks 2 and 3.

Oxidative cyclic voltammograms of $\mathbf{1}^{2+}$ were simulated on the assumption of two quasireversible electron transfers (E) and an irreversible follow-up chemical (C) reaction (EEC mechanism) under linear diffusion conditions. Figure 6 shows simulations with this model and the corresponding experi-

Table 5. Peak potential features in cyclic voltammograms of $\mathbf{1}^{2+}$.

v /V s^{-1}	E_p^7/V			$\lvert E_p^7 - E_{p/2}^7 \rvert$ /V[a]	E_p^2/V[a]	E_p^3/V[a]
	$c = 0.08$	0.18	0.29 mM			
0.01	−0.579	−0.602	−0.602	0.065	+0.361	+0.565
0.02	−0.590	−0.610	−0.613	0.061	+0.362	+0.572
0.05	−0.609	−0.628	−0.633	0.062	+0.364	+0.584
0.1	−0.616	−0.636	−0.643	0.063	+0.364	+0.588
0.2	−0.627	−0.650	−0.657	0.063	+0.360	+0.596
0.5	−0.643	−0.662	−0.675	0.062	+0.362	+0.604
1.0	−0.653	−0.666	−0.681	0.061	+0.360	+0.606
2.0	−0.658	−0.676	−0.688	0.060	+0.362	+0.611
5.12	−0.677	−0.687	−0.703	0.061	+0.367	+0.618
10.24	−0.690	−0.714	−0.741	0.067	+0.372	+0.623
20.48	−0.733	−0.718	−0.734	0.069	+0.379	+0.639
51.2	−0.766	−0.764	−0.772	0.074	+0.391	+0.642

v /V s^{-1}	$\Delta E_p^{2/5}$/V[a]	$\Delta E_p^{3/4}$/V[a]	E_p^1/V		
			$c = 0.08$	0.18	0.29 mM
0.01	0.068	–[b]	−0.155	−0.164	−0.167
0.02	0.067	–[b]	−0.139	−0.147	−0.147
0.05	0.070	–[b]	−0.119	−0.136	−0.122
0.1	0.067	–[b]	−0.104	−0.112	−0.107
0.2	0.064	–[b]	−0.087	−0.097	−0.089
0.5	0.068	–[b]	−0.065	−0.073	−0.068
1.0	0.062	0.074	−0.045	−0.053	−0.052
2.0	0.065	0.072	−0.031	−0.046	−0.039
5.12	0.072	0.068	−0.006	−0.033	−0.017
10.24	0.080	0.070	−0.002	±0.000	+0.014
20.48	0.095	0.095	+0.029	+0.007	+0.017
51.2	0.119	0.108	+0.066	+0.038	+0.070

[a] Independent of c, mean values over data at $c = 0.08$, 0.18, and 0.29 mM. [b] Not observed owing to absence of peak 4.

Table 6. Peak current features in cyclic voltammograms of $\mathbf{1}^{2+}$.

v /V s^{-1}	$i_p^2/\sqrt{v}c$[a]	$i_p^3/\sqrt{v}c$[a,b]	$i_p^7/\sqrt{v}c$[a]	$i_p^1/\sqrt{v}c$[a]	i_p^5/i_p^2	i_p^3/i_p^2[a]
0.01	63	43	96	14	0.94	0.68
0.02	59	43	94	27	0.88	0.72
0.05	56	42	91	37	0.88	0.76
0.1	54	42	92	39	0.90	0.78
0.2	52	43	92	39	0.96	0.82
0.5	51	45	92	36	1.00	0.88
1.0	52	44	92	32	1.00	0.85
2.0	51	45	93	27	1.05	0.89
5.12	56	46	93	22	1.06	0.82
10.24	53	46	92	19	1.17	0.86
20.48	50	45	92	16	1.30	0.90
51.2	46	48	89	14	1.43	1.04

[a] In A s$^{1/2}$ cm^3 V$^{-1/2}$ mol^{-1}, independent of c, mean values over data at $c = 0.08$, 0.18, 0.20, 0.21, 0.29 mM. [b] Determined with extrapolated current from peak 2 as baseline.

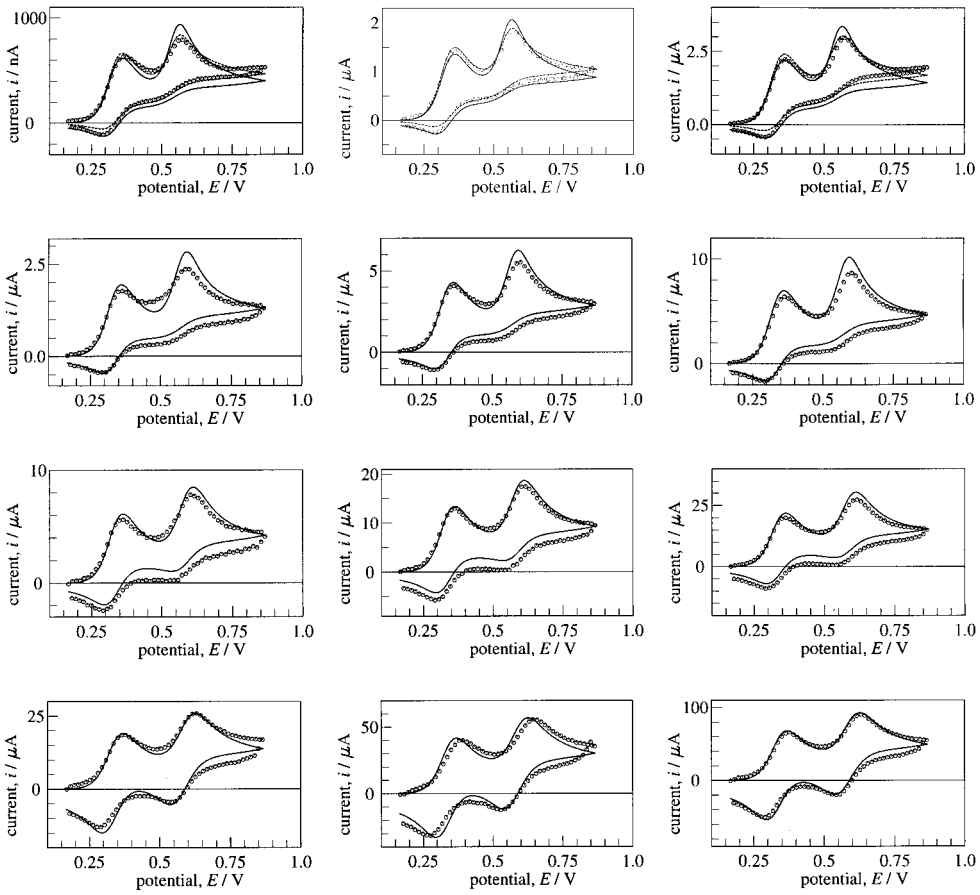

Figure 6. Experimental and simulated cyclic voltammograms of $\mathbf{1}^{2+}$ $(PF_6^-)_2$ in CH_3CN/CH_2Cl_2 (1:1, v/v)/0.1M NBu_4PF_6; symbols: experimental data, solid lines: simulated data, $E^0(\mathbf{1}^{2+}/\mathbf{1}^{3+}) = +0.331$ V, $E^0(\mathbf{1}^{3+}/\mathbf{1}^{4+}) = +0.582$ V, $k_{s,1} = 0.2$ cm s^{-1}, $k_{s,2} = 0.1$ cm s^{-1}, $\alpha_1 = \alpha_2 = 0.5$, $k = 15$ s^{-1}, $D = 8.2 \times 10^{-6}$ cm^2 s^{-1}; conditions in experiments: $c = 0.08$, 0.18, 0.29 mM (left to right), $v = 0.02$, 0.2, 2.0, 20.48 V s^{-1} (top to bottom), $A = 0.071$ cm^2; number of collocation points $N = 9$, spline collocation,[51] expanding simulation space,[52] EEC mechanistic model (CVSIM[50]); additional for curves with $v = 0.02$ V s^{-1}, broken line: simulation with DigiSim including edge diffusion[21] and reaction of $\mathbf{1}^{3+}$ [E(C)EC mechanistic model, rate constant for reaction of trication: $k = 0.07$ s^{-1}].

(Figure 5, solid lines). Peak 7 shifts to more negative, peak 1 to more positive potentials upon an increase in v (Table 5) and at the same time peak 1 broadens considerably. Again, a shift of E_p^7 to more negative potentials with increasing c is noted. The variation of E_p^1 with c that was observed in voltammograms of **1**, on the other hand, is smaller under these conditions. The half-peak potential of peak 7 (Table 5) is almost independent of c as well as v up to 10.24 V s^{-1}. The peak current function of peak 7, $i_p^7/\sqrt{v}c$, does not depend on v. It is therefore confirmed that no adsorption effects are present under the conditions employed here. No decrease of $i_p^7/\sqrt{v}c$ at small v is observed. The diffusional loss of $\mathbf{1}^{2+}$ that we observed starting from **1** at slow scan rates can no longer occur, since now $\mathbf{1}^{2+}$ is the starting species. However, now i_p^1 on the reverse scan shows a nonlinear dependence on $\sqrt{v}$ at slow scan rates. Simulations of the dication reduction voltammograms will be described below.

mental curves for three concentrations of the starting dication and for scan rates varying over three orders of magnitude (0.02 – 20.48 V s^{-1}).

Considering the wide range of experimental parameters used, the experiments can be reproduced by the simulations rather well. Only at small v does edge diffusion tend to influence the experimental curves. At $v = 0.02$ V s^{-1} the fit between experiment and simulation can indeed be increased if we consider the contribution of nonlinear diffusion. Still, peak 3 in the simulations is too intense compared with the experiments. This indicates a slow reaction of $\mathbf{1}^{3+}$, and as a matter of fact, simulations of the E(C)EC mechanistic scheme (rate constant for the reaction of the trication: $k = 0.07$ s^{-1}) further improves the fit at the slowest scan rate shown. Thus, at scan rates above 0.02 V s^{-1} the EEC mechanism with two quasireversible ETs provides a good model for the oxidation of $\mathbf{1}^{2+}$. At $v \leq 0.02$ V s^{-1}, however, an additional reaction of $\mathbf{1}^{3+}$ has to be considered.

Cyclic voltammetry of $\mathbf{1}^{2+}(PF_6^-)_2$; reduction: Initially, peak 1 is not present in cyclic voltammograms of $\mathbf{1}^{2+}$. After the reduction occurring in peak 7, however, oxidation of **1** is observed in peak 1 under cyclic voltammetric conditions

Chronoamperometry and chronocoulometry of $\mathbf{1}^{2+}$ $(PF_6^-)_2$: Oxidative CA and CC experiments (Table 7) in solutions of

Table 7. Chronocoulometric and chronoamperometric results for redox reactions of $\mathbf{1}^{2+}$ at different values of E (in V).[a]

E/V	+0.466	+0.866	−1.134
τ /s			
$Q/\sqrt{tc}$ [b]			
0.1	0.022	0.042	0.055
1.0	0.023	0.042	0.052
10.0	0.027	0.048	0.057
$(Q/\sqrt{tc})/(Q/\sqrt{tc})_{E=+0.166\,V}$			
0.1	1.000	1.90	2.49
1.0	1.000	1.79	2.22
10.0	1.000	1.75	2.09
$Q(2\tau)/Q(\tau)$			
0.1	0.46 ± 0.01	0.66 ± 0.01	0.51 ± 0.05
1.0	0.53 ± 0.02	0.86 ± 0.02	0.49 ± 0.10
10.0	0.69 ± 0.04	0.95 ± 0.04	0.61 ± 0.08
$i/\sqrt{tc}$ [c]	10.6	21.5	22.3
$(i/\sqrt{tc})/(i/\sqrt{tc})_{E=+0.166\,V}$	1.00	2.03	2.10

[a] Mean values from experiments at $c = 0.08$, 0.18, and 0.24 mM. [b] In C cm^3 s$^{-1/2}$ mol^{-1}. [c] In A cm^3 s$^{1/2}$ mol^{-1}, mean values from all τ.

0947-6539/98/0402-0228 $ 17.50+.50/0 Chem. Eur. J. 1998, 4, No. 2

$\mathbf{1}^{2+}$ $(PF_6^-)_2$ are consistent with the stepwise formation of $\mathbf{1}^{3+}$ and $\mathbf{1}^{4+}$ during oxidation (the ratio of electrons transferred was 1:2 for potentials of +0.466 and +0.866 V, respectively), including the hypothesis of the follow-up reaction of the tetracation (increase of $Q(2\tau)/Q(\tau)$ with τ for $E = +0.866$ V, Table 7). Reduction of $\mathbf{1}^{2+}$ also corresponds to the transfer of two electrons according to the Anson slopes and Cottrell constants.

Thermodynamic stability of the oxidation products of 1: The quasireversible two-electron redox process $\mathbf{1} \rightleftharpoons \mathbf{1}^{2+} + 2e^-$ occurs in peak 1, and under the conditions employed in this work the two steps were not separable. Compared with oxidation peak 1, reduction peak 7, corresponding to the reverse reaction $\mathbf{1}^{2+} \rightarrow \mathbf{1}$, is strongly shifted to negative potentials; this suggests inversion of the formal potentials characterizing the two one-electron processes $\mathbf{1} \rightleftharpoons \mathbf{1}^{\bullet+} + e^-$ and $\mathbf{1}^{\bullet+} \rightleftharpoons \mathbf{1}^{2+} + e^-$; that is, the one-electron redox potential of **1**, $E^0(\mathbf{1}/\mathbf{1}^{\bullet+})$, is more positive than $E^0(\mathbf{1}^{\bullet+}/\mathbf{1}^{2+})$. In a cyclic voltammogram starting from **1** (see Figure 2, for example), an electrode process could only occur if the electrode potential were positive enough to trigger reaction $\mathbf{1} \rightarrow \mathbf{1}^{\bullet+} + e^-$.

We could find no experimental evidence to decide whether a hypothetical radical cation $\mathbf{1}^{\bullet+}$ is at all stable, since as soon as it were formed, it would be further oxidized, either heterogeneously at the electrode or by homogeneous disproportionation according to Equation (i). This equilibrium is shifted to

$$2\mathbf{1}^{\bullet+} \rightleftharpoons \mathbf{1} + \mathbf{1}^{2+} \quad \text{(i)}$$

the right if inversion of potentials occurs. On the reverse scan, reduction starts from $\mathbf{1}^{2+}$ and can only be observed if the electrode potential is negative enough for the step $\mathbf{1}^{2+} + e^- \rightarrow \mathbf{1}^{\bullet+}$ to be feasible. Inversion of potentials results in rather negative values of E_p^7. Again, either heterogeneous reduction or disproportionation of the hypothetical radical cation occurs and yields **1**.

Inversion of potentials implies[27] that the energetic difference between the first (here radical cation $\mathbf{1}^{\bullet+}$) and the second oxidation stage (in the present case $\mathbf{1}^{2+}$) is smaller than the one between the starting compound **1** and $\mathbf{1}^{\bullet+}$. Evans and Hu[27] have related inversion of potentials in the case of hydrocarbon reduction to the facts that a) both electron-transfer products (radical anion and dianion in their case) are stabilized if they attain their own structure as compared with the situation in which they retain the structure of the neutral starting compound and b) this effect is much stronger for the product of the second ET than that of the first. In the present system, inversion of the redox potentials could be explained by the fact that **1** undergoes considerable structural changes during oxidation. Although X-ray analysis of $\mathbf{1}^{2+}$ $(PF_6^-)_2$ yields the structure of the dication in the solid state only, it has been shown that at least for the corresponding bis(triiodide) the dication has a twisted structure in solution too.[2] The solution NMR spectra of the dication salts are almost identical and it is thus reasonable to assume the same relation for the solid-state and solution structures of the bis(hexafluorophosphate) of $\mathbf{1}^{2+}$. In such a twisted conformation, stabilization can be expected as a result of the formation of two polymethine systems in the dication,[30] which is confirmed in the solid state by the bond lengths (C_1-N_{11} and C_3-N_{31} shortened compared with C_2-N_{21}) and at least for $\mathbf{1}^{2+}$ $(I_3^-)_2$ in solution by dynamic NMR results.[2] Therefore, we propose that stabilization of $\mathbf{1}^{2+}$ through structural changes makes its formation from $\mathbf{1}^{\bullet+}$ thermodynamically easier than the formation of $\mathbf{1}^{\bullet+}$ from the neutral starting species **1**. As a result, the order of the formal potentials of successive oxidation states linked by two sequential ETs (commonly separated by about +0.4 V[31]) is reversed. This is in direct contrast to the earlier reasoning,[1–4] which assumed a *destabilization* of the dication. Energetic stabilization of polymethine systems by delocalization has been characterized as between that of aromatic compounds and polyenes.[32]

In accordance with the conclusion from Equation (i) considering inversion of potentials, an ESR spectrum unequivocally assigned to $\mathbf{1}^{\bullet+}$ could not yet be detected in solution.[20] Electronic spectra also confirm a shift of Equilibrium (i) far over to the right-hand side. The UV/Vis spectrum (Figure 7) of neutral **1** does not show a maximum

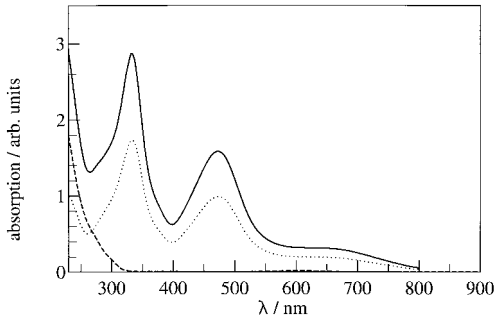

Figure 7. UV/Vis spectra of **1**, $c = 0.255$ mM (- - -), of $\mathbf{1}^{2+}$, $c = 0.136$ mM (···), and of a mixture of **1** and $\mathbf{1}^{2+}$, $c(\mathbf{1}) = c(\mathbf{1}^{2+}) = 0.182$ mM (—), in CH_3CN/CH_2Cl_2 (1:1, v/v).

in the accessible range of wavelengths ($230 \le \lambda \le 800$ nm) in CH_3CN/CH_2Cl_2 (1:1), while the dication has a spectrum with two clearly defined maxima [$\lambda_{max} = 334$ nm, $\varepsilon = (1.3 \pm 0.1) \times 10^4$; $\lambda_{max} = 334$ nm, $\varepsilon = (7.2 \pm 0.7) \times 10^3$] and a weak shoulder around 620 nm [$\varepsilon = (1.5 \pm 0.2) \times 10^3$]. The spectrum of an equimolar mixture of **1** and $\mathbf{1}^{2+}$ is an exact superimposition of the spectra of hexakis(dimethylamino)benzene and its dication. At least in the wavelength range investigated, no additional bands show up. This makes presence of a radical cation in substantial concentrations rather unlikely.

In this context it is interesting to note that potential inversion has also been observed to various degrees in the case of pyridyl-substituted cyclobutanes.[33] In a 1,3-bismethylenecyclobutane/bicyclo[1.1.0]butane system the redox process was characterized as an ECE-type sequence.[34] In these cases, however, only a single polymethine unit was contained in the molecule, while in the present example of $\mathbf{1}^{2+}$ *two* such units are linked.

In contrast to the case of **1** and $\mathbf{1}^{2+}$, the stability of $\mathbf{1}^{3+}$ and $\mathbf{1}^{4+}$ follows the normal pattern: oxidation becomes more difficult with increasing positive charge on the ions. We have no experimental information on the structure of these higher oxidation products of **1**. Normal ordering of potentials,

however, suggests that structural changes accompanying these oxidation steps are of minor importance. Possibly the central $(CH_3)N_2$ groups in the two polymethine moieties, which are not included in the delocalized systems of the dication (nitrogen atoms N21 and N51 in Figure 4), now bear the additional charge(s).

Determination of $E^0(\mathbf{1}/\mathbf{1}^{2+})$: Recently, Hu and Evans[21] showed that the mean value of the E^0 of an inverted two-electron system is accessible from potentiometric experiments. The equilibrium potential of an indicator electrode is determined in the presence of various concentrations of the two redox partners. In their case, one partner of the redox couple was used as the starting compound, and the other one was generated by electrolysis. The amount of product formed was determined from the charge passed through the electrode. The resulting E^0 characterizes the overall thermodynamics of the two-electron system.

In the case of **1** and $\mathbf{1}^{2+}$, both redox partners are stable and can be prepared in pure form. Thus, $E^0(\mathbf{1}/\mathbf{1}^{2+}) = [E^0(\mathbf{1}/\mathbf{1}^{\bullet+}) + E^0(\mathbf{1}^{\bullet+}/\mathbf{1}^{2+})]/2$ is accessible from equilibrium potential measurements in solutions with various ratios $[\mathbf{1}]/[\mathbf{1}^{2+}]$, which were prepared by mixing stock solutions of the two species. Results are plotted in Figure 8 versus the ratio $x_{\mathbf{1}^{2+}} = [\mathbf{1}^{2+}]/([\mathbf{1}^{2+}] + [\mathbf{1}])$

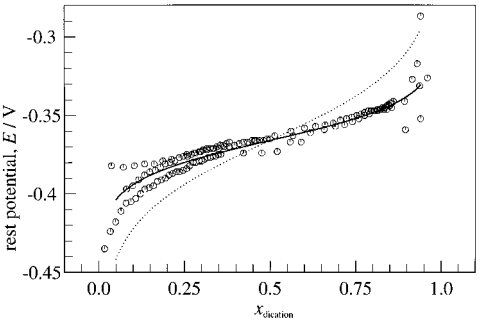

Figure 8. Equilibrium potential of a Pt tip electrode in solutions of **1** and $\mathbf{1}^{2+}$ in CH_3CN/CH_2Cl_2 (1:1, v/v)/0.1M NBu_4PF_6 as a function of $x_{\mathbf{1}^{2+}}$ (see text for definition); symbols: data from three independent experiments; theoretical curves for $E^0(\mathbf{1}/\mathbf{1}^{2+}) = -0.366$ V, solid line: $n = 2$, dotted line: $n = 1$.

and compared with a theoretical curve (solid line) calculated according to Equation (1) (derived from the Nernst equation,

$$E = E^0(\mathbf{1}/\mathbf{1}^{2+}) - \frac{RT}{nF}\ln\left(\frac{1}{x_{\mathbf{1}^{2+}}} - 1.0\right) \quad (1)$$

$n = 2$, $T = 298$ K, R being the gas constant and F the Faraday) with $E^0(\mathbf{1}/\mathbf{1}^{2+}) = -0.366$ V. Good agreement is found for a series of independent experiments. A theoretical curve with $n = 1$ (dotted line) does *not* fit the experimental data well. Only at the extreme limits of small and large $x_{\mathbf{1}^{2+}}$ does scatter of the experimental data occur, probably due to uncertainties in the concentration of the two redox partners. The results provide an estimate of the overall redox potential $\mathbf{1} \rightarrow \mathbf{1}^{2+} + 2\,e^-$.

Kinetics of electrode reaction $\mathbf{1} \rightleftharpoons \mathbf{1}^{2+}$: The peak potential difference between peaks 1 and 7 and the dependence of the half-peak width $|E_p^1 - E_{p/2}^1|$ (Table 1) on the scan rate indicate that, in addition to inversion of the formal potentials, the overall redox process is kinetically slow. Two fully reversible ET processes would result in a peak potential difference of 29 mV with $E = E^0(\mathbf{1}/\mathbf{1}^{2+})$ even if the formal potentials were inverted, and a half-peak width of 29 mV. Furthermore, for reversible ETs, the peak potentials E_p^1 and E_p^7 were expected to be independent of v.

Sluggish ET may be brought about by a structural change of the molecule during the redox reaction, concerted with at least one of the heterogeneous steps.[21] This would correspond to a large inner reorganization energy λ_i during the oxidation. It has recently been shown that effects of λ_i and those of a bond dissociation concerted with the ET on the activation barrier are similar for *one*-electron transfer processes.[35–37] The present case of a two-electron system, however, is much more complicated due to the larger number of alternative reaction pathways. For example, the structural change could be nonconcerted with any of the electron transfers and happen either at the radical cation or the dication stage, or it could be concerted with either of the ET steps. Furthermore, considerable changes in the molecular structure may occur during *both* of the two ET processes. Finally, even the two ETs may be concerted into a single elementary reaction. A detailed kinetic analysis of the reaction $\mathbf{1} \rightleftharpoons \mathbf{1}^{2+} + 2\,e^-$ must therefore await further theoretical development.[38]

Simulations for an EE reaction with inversion of potentials, a fast (diffusion-controlled) homogeneous disproportionation reaction of $\mathbf{1}^{\bullet+}$, slow ET kinetics for both steps, *and* potential-dependent transfer coefficients α, however, already show that the overall shape of the voltammograms in the system $\mathbf{1}/\mathbf{1}^{2+}$ can be reproduced. Simulations of an ECE process were less successful. Formulation as an EE reaction implies that structural changes are concerted with one or both electron transfers. In particular, the fact that at large scan rates the half-peak widths of peaks 1 and 7 are different, with peak 1 being more drawn out than peak 7 (see Tables 1 and 5 and Figure 2c), shows up in the simulations. Also, a concentration-dependent shift of the peak potentials, probably due to the influence of the second-order disproportionation, can be seen in these simulations. Future work will be directed at providing a more quantitative picture of the two-electron oxidation of **1**.

Oxidation mechanism of 1 and comparison with other aminobenzenes: Hexakis(dimethylamino)benzene **1** was oxidized in three steps in the CH_3CN/CH_2Cl_2 electrolyte, yielding di-, tri-, and tetracations (Scheme 1). The experimental data prove oxidation in a quasireversible two-electron step and two faster, successive separate one-electron steps with follow-up reactions at the tri- and tetracation stages. The two voltammetric peaks corresponding to the primary redox reaction are, however, separated by more than 0.5 V, because of the combined effects of inversion of the formal potentials (thermodynamics) and the sluggishness of at least one of the electron transfers (kinetics).

Dietrich and Heinze also observed a three-step oxidative cyclic voltammogram of **1** in liquid SO_2 and CH_2Cl_2,[4] but at much more positive potentials than in our work

  0947-6539/98/0402-0230 $ 17.50+.50/0 *Chem. Eur. J.* **1998**, *4*, No. 2

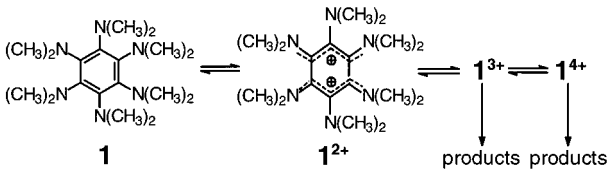

Scheme 1. Oxidation mechanism of hexakis(dimethylamino)benzene in CH_3CN/CH_2Cl_2.

(+0.31, +0.56, and +1.64 V vs. fc/fc$^+$, recalculated from values vs. Ag/AgCl with the ferrocene potential given in ref. [4]). Surprisingly, for increasing E their data correspond to two separate *one*-electron transfers followed by a *two*-electron process.[39] This result can be reconciled with our data if we assume that in their system $\mathbf{1}^{2+}$ was present as the starting compound (possibly due to oxidation by the solvent SO_2). Indeed, the E^0 values for their first two steps are almost identical to the formal potentials for tri- and tetracation formation determined in the present work. Their third wave would then correspond to *hexa*cation formation. The potential of this wave lies outside the potential window accessible in CH_3CN/CH_2Cl_2 under the conditions used in the present work, precluding formation of such a highly charged species.

N,*N*,*N*′,*N*′-Tetramethyl-*p*-phenylenediamine (**5**), one of the best-investigated aromatic amino compounds as regards its electron transfer properties, is oxidized in the CH_3CN/CH_2Cl_2 electrolyte at $E^0 = -0.292 \pm 0.002$ and $E^0 = -0.343 \pm 0.003$ V in two one-electron steps via its radical cation (Wurster's Blue[40]) to its dication [values in pure acetonitrile: −0.206 and +0.378 V,[5] −0.207 and +0.373 V (recalculated vs. fc/fc$^+$ from ref. [7]), −0.27 and +0.33 V;[6] for a recent investigation of solvent effects on $E^0(\mathbf{5}/\mathbf{5}^{\bullet+})$, see ref. [41]]. The mean value of these two formal potentials, $E^0(\mathbf{5}/\mathbf{5}^{2+}) = [E^0(\mathbf{5}/\mathbf{5}^{\bullet+}) + E^0(\mathbf{5}^{\bullet+}/\mathbf{5}^{2+})]/2 = +0.026$ V, can be compared to $E^0(\mathbf{1}/\mathbf{1}^{2+}) = -0.366$ V, since both E^0 describe an overall two-electron process. **1** is oxidized considerably more easy than **5**.

Another compound suitable for direct comparison with **1** with respect to the oxidation potential is 1,2,4,5-tetrakis(dimethylamino)benzene (**2**). The formal potential for the two-electron oxidation of **2** in acetonitrile is −0.266 V vs. fc/fc$^+$,[5] 0.1 V more positive than $E^0(\mathbf{1}/\mathbf{1}^{2+})$. Comparison of the oxidation potentials of **1**, **2**, and **5** reveals that that of **1** is not unusually high.

It is interesting to note, however, that in contrast to most of the other dimethylamino-substituted benzenes or their derivatives, **1** shows both inversion of potentials and a small heterogeneous electron transfer rate. As such its electrochemical behavior is indeed different from most similar compounds, for example **5**–**8**. In the absence of quantitative kinetic data for the oxidation of **1**, the reason for this difference will be discussed qualitatively here. It does appear that this behavior is not simply related to the fact that a structural change occurs at all during oxidation, or that steric strain occurs in the oxidation product.

One would expect strong steric effects in the HOC dication $\mathbf{8}^{2+}$ because of the ethano bridges linking the nitrogen atoms in this coronene derivative. Dication $\mathbf{8}^{2+}$ is described as having an essentially planar C_6N_6 core,[17] but forms two polymethine moieties. The central six-membered ring now consists of two C_3 units with short C–C bonds. The units are connected by two long C–C single bonds. These structural features are similiar to $\mathbf{1}^{2+}$. In contrast to the HDMAB dication, however, the polymethine systems in $\mathbf{8}^{2+}$ are held coplanar by the ethano framework. In contrast to **8**, the C–C bond lengths in the HOC dication are no longer equal. Consequently, there is indeed a considerable change of the molecular structure in going from **8** to $\mathbf{8}^{2+}$, but confined to the planar core ring. The cyclic voltammogram of **8** shows four *reversible one-electron* peak couples and none of the effects discussed for **1**. 1,2,4,5-Tetrakis(dimethylamino)benzene (**2**), on the other hand, shows inversion of potentials: its two-electron oxidation peak could not be separated into two one-electron signals.[5] Its voltammogram was not analyzed with regard to the kinetics of the ET,[5] but its peak potential separation is clearly increased above the 29 mV expected for a reversible system, indicating slow heterogeneous ET.

The main difference between the systems $\mathbf{1}/\mathbf{1}^{2+}$ and $\mathbf{2}/\mathbf{2}^{2+}$ on the one hand and $\mathbf{8}/\mathbf{8}^{2+}$ on the other is the fact that the structural distortion in $\mathbf{1}^{2+}$ and $\mathbf{2}^{2+}$ (compared with **1** and **2**, respectively) is out-of-plane and that the polymethine systems are no longer coplanar but tilted relative to each other. We suggest that this particular feature of the structural change during ET contributes to stabilization of $\mathbf{1}^{2+}$ and $\mathbf{2}^{2+}$ compared with hypothetical dications with a structure not much different from the neutral parent (i.e. with parallel polymethine units), and may be responsible for the effects which we observe experimentally. In particular, stabilization explains the inversion of potentials in these cases. Dication $\mathbf{8}^{2+}$ does not have this stabilizing feature, and its polymethine units must remain coplanar. Thus, normal ordering of potentials is observed. This hypothesis could possibly be tested through detailed analysis of the redox properties of other polyaminobenzenes with various degrees and types of steric restraints.

In future experiments, we will therefore extend our experiments to HDMAB derivatives with cyclophane-type rings linking two nitrogen atoms in *meta* positions to those with a $NH(CH_3)$ group replacing *one* dimethylamino substituent, and to those with two hexaaminobenzene moieties linked by aliphatic spacer units (see for example ref. [42]).

Experimental Section

General: Hexakis(dimethylamino)benzene was synthesized according to published procedures from 1,3,5-trichloro-2,4,6-trinitrobenzene via 1,3,5-triamino-2,4,6-trinitrobenzene and hexaaminobenzene.[43] Elemental analyses were performed in the Chemisches Zentralinstitut (Universität Tübingen). Nuclear magnetic resonance spectra were recorded on a Bruker AC250 spectrometer.

Solvents and supporting electrolytes: Dichloromethane was predried over $CaCl_2$. It was distilled from P_2O_5 and then K_2CO_3, and passed through an Al_2O_3 column (diameter: 2 cm, length: 15 cm; neutral alumina, dried at 140 °C and cooled under argon). Acetonitrile was predried over $CaCl_2$. It was distilled from P_2O_5, NaH and again P_2O_5, and passed through an Al_2O_3 column as described above. Tetra-*n*-butylammonium hexafluorophosphate, NBu_4PF_6, was prepared from NBu_4Br and NH_4PF_6 or recycled as described before.[44] It was used in a concentration of 0.1 M in the respective solvent. The electrolyte was degassed by three freeze–pump–thaw cycles before it was transferred into the electrochemical cell under argon.

Electrochemical experiments: All electrochemical experiments were performed with a Bioanalytical Systems (BAS, West Lafayette, IN, USA) 100 B/W electrochemical workstation controlled by a standard 80486 personal computer (control program version 2.0). For electroanalytical experiments a Metrohm Pt electrode tip (Filderstadt, Germany) was used as working electrode. The electroactive area of the Pt disk was determined from cyclic voltammograms, chronoampero- and chronocoulograms of ferrocene (fc) in acetonitrile, CH_2Cl_2 and a 1:1 (v/v) mixture of these solvents to be $A = 0.071 \pm 0.007$ cm^2, with diffusion coefficients D for fc in CH_3CN (2.4×10^{-5} cm^{2}s^{-1})[45] and CH_2Cl_2 (2.32×10^{-5} cm^{2}s^{-1}).[46] The value of D in the solvent mixture was calculated as the mean value of the values in the pure solvents. The counterelectrode was a Pt wire of 1 mm diameter. A single-unit Haber–Luggin double-reference electrode[47] was used. The resulting potential values refer to Ag/Ag^+ (0.01 M in CH_3CN/0.1 M NBu_4PF_6). Ferrocene was used as an external standard. Its potential was determined by separate cyclic voltammetric experiments in the respective solvent, and all potentials were then rescaled to E^0(fc/fc$^+$) (+0.093 V in CH_3CN, +0.211 V in CH_2Cl_2, and +0.134 V in the CH_3CN/CH_2Cl_2 electrolyte, all vs. Ag/Ag^+). All potentials in the present paper are reported relative to the fc/fc$^+$ standard[48] in the respective solvent.

For cyclic voltammetry, chronoamperometry, chronocoulometry, and potentiometry a gas-tight full-glass three-electrode cell was used; its assembly for the experiments has been described previously.[44] The cell was purged with argon before it was filled with electrolyte. Except for the potentiometric determinations, background curves were recorded before adding substrate to the solution. These were later subtracted from the experimental data with substrate. The automatic BAS 100 B/W *iR*-drop compensation facility was used for all experiments.

For preparative electrolyses working and counterelectrodes were nets of Pt/Ir 90/10 (Degussa, Hanau, Germany), separated by a glass frit. The reference electrode was identical to the one described above. The cell was fitted with an additional Pt tip electrode (see above) to record cyclic voltammograms. This cell was also gas-tight and its temperature could be held constant. It was purged with argon prior to being filled with electrolyte.

Numerical simulations[49] were performed with our CVSIM package[50] on a CONVEX C3860 mainframe computer. The programm uses spline orthogonal collocation[51] with the expanding simulation space option[52] and was extended to accommodate the electrode reaction mechanisms encountered in the present work. In particular the possibility of using a potential-dependent transfer coefficient α for quasireversible ET processes was included, according to Equation (2). Additional simulations to include edge diffusion (empirical procedure as given in ref. [21]) and trication reaction used the commercial simulator Digisim.[53]

$$\alpha = \alpha_0 + (E - E^0)\frac{d\alpha}{dE} \qquad (2)$$

Preparative electrolysis of 1; preparation of $\mathbf{1}^{2+}(\mathbf{PF_6^-})_2$: A 0.1 M solution of NBu_4PF_6 in CH_2Cl_2 (20 mL) was placed in the working electrode compartment of the electrolysis cell. The counterelectrode compartment was filled with the same electrolyte. After inserting the double-reference electrode with the Haber–Luggin capillary and stabilizing the cell temperature at 17 °C, **1** (67.4 mg, 0.2 mmol) was dissolved in the electrolyte in the working electrode compartment and a cyclic voltammogram was recorded with the tip electrode. Then the solution was electrolyzed at $E = +0.289$ V, until the primary oxidation peak of **1** in the voltammograms had disappeared. A charge of 39.4 C (expected for $n = 2$: 38.6 C) had passed. A precipitate had formed in the working electrode compartment. It was filtered off and dried at ambient temperature and 5×10^{-2} mbar to yield 52.5 mg $\mathbf{1}^{2+}(PF_6^-)_2$ (42 %). $C_{18}H_{36}F_{12}N_6P_2$ (626.47): calcd C 34.51, H 5.79, N. 13.42, F 36.39; found C 34.26, H 5.64, N, 12.71, F 37.02; ^{1}H NMR (200 MHz, [D$_6$]DMSO, TMS): $\delta = 3.07$ (s); ^{1}H NMR (200 MHz, CD_2Cl_2, TMS): $\delta = 3.15$ (s) ($\mathbf{1}^{2+}(I_3^-)_2$: 3.30 (s) in CD_2Cl_2, see ref. [2]); ^{13}C NMR (200 MHz, [D$_6$]DMSO, TMS): $\delta = 44.09$ (CH_3), 144.05 (ring carbon atoms) ($\mathbf{1}^{2+}(I_3^-)_2$: $\delta = 44.08$, 143.92 in [D$_6$]DMSO, see ref. [2]).

Potentiometric determination of equilibrium potential $\mathbf{E^0(1/1^{2+})}$: The equilibrium potentials[21] of solutions containing both **1** and $\mathbf{1}^{2+}$ were determined as the rest potentials of a Pt electrode in the electrolyte. Typical experiment: Two stock solutions were prepared, one with 3.91 mg and the other with 39.48 mg of $\mathbf{1}^{2+}$, in the electrolyte [CH_3CN/CH_2Cl_2, 1:1 (v/v) with 0.1 M NBu_4PF_6]. Compound **1** (0.48 mg) was dissolved in the electrolyte (20 mL). Several portions of the dication solutions were added, and each time the rest potential was determined with the BAS 100 B/W. Determinations with a fixed concentration ratio of **1** and $\mathbf{1}^{2+}$ were repeated until the rest potential stayed constant. Between the determinations the solution was stirred for 2 min. The rest potential was plotted versus the concentration ratio $x_{\mathbf{1}^{2+}} = [\mathbf{1}^{2+}]/([\mathbf{1}^{2+}] + [\mathbf{1}])$. The value of $E^0(\mathbf{1}/\mathbf{1}^{2+})$ follows as the point of inflection of the plot or from comparison with curves calculated from Equation (1).

UV/Vis spectra: A recording spectral photometer Specord M 500, Zeiss, Jena (Germany), was used with 1 cm pathlength quartz cuvettes. The reference was the pure solvent and the concentrations were chosen such that the extinction was between 0.1 and 0.15. The extinction was plotted vs. the concentration and the extinction coefficient determined from the slope of the resulting straight line.

Crystal structure determination: Crystals of the dication bis(hexafluorophosphate) were obtained by slow diffusion of diethyl ether into a solution of the salt in acetonitrile. The X-ray data were collected with an Enraf–Nonius diffractometer. Crystal data are reported in Table 8. The data were collected with θ ranging from 5.6 to 65; there were 4912 reflections, of which 4489 with $I > 2\sigma$ have been used for the structure determination. The structure was solved by direct methods[54] and refined by the full-matrix least-squares method.[55] Refinement of the model with anisotropic temperature parameters and the hydrogen atoms calculated on ideal positions led to an R value of 0.085, with highly disordered PF_6^- ions.

Table 8. Crystal data and structure refinement for $\mathbf{1}^{2+}$.

formula	$C_{18}H_{36}F_{12}N_6P_2$
M_r	626.47
T	293(2) K
λ/radiation	1.54056 Å/$Cu_{K\alpha}$
crystal system/space group	orthorhombic/*Pbca*
unit cell dimensions:	
a	18.972(2)
b	12.6050(14)
c	22.8100(12)
V	5454.8(9) Å^3
Z	8
ρ_{calcd}	1.526 Mg m^{-3}
absorption coefficient	2.408 mm^{-1}
$F(000)$	2592
crystal size	0.6 × 0.2 × 0.15 mm
index ranges	$0 \le h \le 22$, $-1 \le k \le 14$, $-23 \le l \le 0$
reflections collected	4912
independent reflections	4489 [R(int) = 0.0346]
reflections observed	3285
criterion for observation	$> 2\sigma(I)$
absorption correction	none
data/restraints/parameters	4489/0/347

Crystallographic data (excluding structure factors) for the structure reported in this paper have been deposited with the Cambridge Crystallographic Data Centre as supplementary publication no. CCDC-100296. Copies of the data can be obtained free of charge on application to CCDC, 12 Union Road, Cambridge CB2 1EZ, UK (Fax: int. code + (44) 1223 226-033; e-mail: deposit@ccdc.cam.ac.uk).

Acknowledgments: We thank the Deutsche Forschungsgemeinschaft, the Fonds der Chemischen Industrie, and the Land Baden–Württemberg (program Molekulare Elektrochemie) for financial support. B.S. gratefully acknowledges the award of a Heisenberg fellowship. We are grateful to J. J. Wolff (Heidelberg) for gifts of samples and many discussions, to J.-M. Savéant (Paris) and J. Heinze (Freiburg) for discussions, K. Mislow (Princeton) for providing us with details of the $\mathbf{1}^{2+}(I_3^-)_2$ structural analysis, G. Gauglitz and U. Schobel (Tübingen) for the use of their UV/Vis spectrometer, and R. Mayer for preliminary CV experiments on **1**.

Received: April 9, 1997 [F 665]

[1] J. Thomaides, P. Maslak, R. Breslow, *J. Am. Chem. Soc.* **1988**, *110*, 3970–3979.
[2] J. M. Chance, B. Kahr, A. B. Buda, J. P. Toscano, K. Mislow, *J. Org. Chem.* **1988**, *53*, 3226–3232.
[3] R. W. Johnson, *Tetrahedron Lett.* **1976**, 589–592.
[4] M. Dietrich, J. Heinze, *J. Am. Chem. Soc.* **1990**, *112*, 5142–5145.
[5] K. Elbl, C. Krieger, H. A. Staab, *Angew. Chem.* **1986**, *98*, 1024–1026; *Angew. Chem. Int. Ed. Engl.* **1986**, *25*, 1023–1024.
[6] K. Hu, D. H. Evans, *J. Electroanal. Chem.* **1997**, *423*, 29–35.
[7] T. Yao, S. Musha, M. Munemori, *Chem. Lett.* **1974**, 939–944.
[8] P. J. Kinlen, D. H. Evans, S. F. Nelsen, *J. Electroanal. Chem.* **1979**, *97*, 265–281.
[9] M. Yano, K. Sato, D. Shiomi, A. Ichimura, K. Abe, T. Takui, K. Itoh, *Tetrahedron Lett.* **1996**, *37*, 9207–9210.
[10] L. Y. Chiang, R. B. Upasani, D. P. Goshorn, P. Tindall, in *Mater. Res. Soc. Symp. Proc. 173 (Adv. Org. Solid State Mater.)*, 15–25, **1990**.
[11] K. R. Stickley, S. C. Blackstock, *J. Am. Chem. Soc.* **1994**, *116*, 11576–11577.
[12] K. R. Stickley, S. C. Blackstock, *Mol. Cryst. Liq. Cryst.* **1995**, *272*, 81–85.
[13] K. R. Stickley, S. C. Blackstock, *Tetrahedron Lett.* **1995**, *36*, 1585–1588.
[14] S. Sasaki, M. Iyoda, *Mol. Cryst. Liq. Cryst.* **1995**, *272*, 175–182.
[15] D. A. Dixon, J. C. Calabrese, J. S. Miller, *Angew. Chem.* **1989**, *101*, 79–81; *Angew. Chem. Int. Ed. Engl.* **1989**, *28*, 90–92.
[16] R. Breslow, P. Maslak, J. S. Thomaides, *J. Am. Chem. Soc.* **1984**, *106*, 6453–6454.
[17] J. S. Miller, D. A. Dixon, J. C. Calabrese, C. Vazquez, P. J. Krusic, M. D. Ward, E. Wasserman, R. L. Harlow, *J. Am. Chem. Soc.* **1990**, *112*, 381–398.
[18] M. Cariou, T. Douadi, J. Simonet, *Bull. Soc. Chim. Fr.* **1996**, *133*, 597–610.
[19] R. B. Upasani, L. Y. Chiang, D. P. Goshorn, P. Tindall, *Mol. Cryst. Liq. Cryst.* **1990**, *190*, 35–43.
[20] G. Gescheidt, Basel, personal communication.
[21] K. Hu, D. H. Evans, *J. Phys. Chem.* **1996**, *100*, 3030–3036.
[22] K. Hu, M. E. Niyazymbetov, D. H. Evans, *J. Electroanal. Chem.* **1995**, *396*, 457–464.
[23] M. Dietrich, J. Heinze, C. Krieger, F. A. Neugebauer, *J. Am. Chem. Soc.* **1996**, *118*, 5020–5030.
[24] B. Brielbeck, J. C. Rühl, D. H. Evans, *J. Am. Chem. Soc.* **1993**, *115*, 11898–11905.
[25] S. F. Nelsen, *Adv. Electr. Transf. Chem.* **1993**, *3*, 167–189.
[26] S. F. Nelsen, H. Chang, J. J. Wolff, J. Adamus, *J. Am. Chem. Soc.* **1993**, *115*, 12276–12289.
[27] D. H. Evans, K. Hu, *J. Chem. Soc. Faraday Trans.* **1996**, *92*, 3983–3990.
[28] A. J. Bard, L. R. Faulkner, *Electrochemical Methods: Fundamentals and Applications*, John Wiley, New York, **1980**, p. 138 ff.
[29] Ref. [28], p. 203.
[30] S. Dähne, D. Leupold, *Angew. Chem.* **1966**, *78*, 1029–1039; *Angew. Chem. Int. Ed. Engl.* **1966**, *5*, 984–993.
[31] J. Phelps, A. J. Bard, *J. Electroanal. Chem.* **1976**, *68*, 313–335.
[32] S. Dähne, *Chimia* **1991**, *45*, 288–296.
[33] M. Horner, S. Hünig, *Liebigs Ann. Chem.* **1983**, 642–657.
[34] M. Horner, S. Hünig, *J. Am. Chem. Soc.* **1977**, *99*, 6122–6124.
[35] J.-M. Savéant, *J. Am. Chem. Soc.* **1987**, *109*, 6788–6795.
[36] J.-M. Savéant, *J. Am. Chem. Soc.* **1992**, *114*, 10595–10602.
[37] J.-M. Savéant, *Acc. Chem. Res.* **1993**, *26*, 455–461.
[38] J.-M. Savéant, Paris, personal communication.
[39] J. Heinze, Freiburg, personal communication.
[40] H. D. Roth, *Tetrahedron* **1986**, *42*, 6097–6100.
[41] M. B. Moressi, M. A. Zón, H. Fernández, *Electrochim. Acta* **1997**, *42*, 303–314.
[42] J. J. Wolff, A. Zietsch, H. Irngartinger, T. Oeser, *Angew. Chem.* **1997**, *109*, 637–639; *Angew. Chem. Int. Ed. Engl.* **1997**, *36*, 621–623.
[43] J. J. Wolff, H.-H. Limbach, *Liebigs Ann. Chem.* **1991**, 691–693.
[44] S. Dümmling, E. Eichhorn, S. Schneider, B. Speiser, M. Würde, *Curr. Sep.* **1996**, *15*, 53–56.
[45] T. Kuwana, D. E. Bublitz, G. Hoh, *J. Am. Chem. Soc.* **1960**, *82*, 5811–5817.
[46] J. B. Cooper, A. M. Bond, *J. Electroanal. Chem.* **1991**, *315*, 143–160.
[47] B. Gollas, B. Krauß, B. Speiser, H. Stahl, *Curr. Sep.* **1994**, *13*, 42–44.
[48] G. Gritzner, J. Kůta, *Pure Appl. Chem.* **1984**, *56*, 461–466.
[49] B. Speiser, in *Electroanalytical Chemistry, Vol. 19* (Eds.: A. J. Bard, I. Rubinstein), Marcel Dekker, New York, **1996**, p. 1–108.
[50] B. Speiser, *Comput. Chem.* **1990**, *14*, 127–140.
[51] P. Hertl, B. Speiser, *J. Electroanal. Chem.* **1987**, *217*, 225–238.
[52] P. Urban, B. Speiser, *J. Electroanal. Chem.* **1988**, *241*, 17–31.
[53] M. Rudolph, D. P. Reddy, S. W. Feldberg, *Anal. Chem.* **1994**, *66*, 589A–600A.
[54] G. M. Sheldrick, SHELXS-86, Program for solving crystal structures, University of Göttingen, **1986**.
[55] G. M. Sheldrick, SHELXL-93, Program for refining crystal structures, University of Göttingen, **1993**.

  0947-6539/98/0402-0233 $ 17.50+.25/0